ChemComm

COMMUNICATION

View Article Online
View Journal | View Issue

Cite this: *Chem. Commun.*, 2023, **59**, 1967

Received 24th November 2022,
Accepted 27th December 2022

DOI: 10.1039/d2cc06368a

rsc.li/chemcomm

Ring-shaped self-assembly of a naphthalene-linked chlorophyll dimer†

Tatsuma Ishii,[a] Shogo Matsubara *[ab] and Hitoshi Tamiaki *[a]

Light-harvesting antennas, for example the LH2 complex in purple bacteria, sophisticatedly align chlorophyll molecules in a cyclic fashion by using protein scaffolds. However, artificial preparation of the circular LH antenna model without any templates has not been reported. We demonstrated the construction of ring-shaped supramolecules by self-assembly of a semisynthetic chlorophyll dimer through a transformation from wavy fiber-like aggregates.

Photosynthetic light-harvesting (LH) antennas densely and orderly array various pigments to absorb sunlight efficiently.[1,2] Their circular arrangements are often found in the LH systems. For instance, chlorophyll pigments in LH1 and LH2 of purple photosynthetic bacteria are arranged to form ring-shaped architectures by using protein scaffolds.[3–6] In major LH antennas of green photosynthetic bacteria called chlorosomes, chlorophyll molecules assemble in a circle-like and spiral fashion to construct tubular supramolecular aggregates.[7,8] These self-assemblies enable efficient sunlight absorption and excitation energy migration and transfer.[9–11] Mimicking such an array of pigments is critical to understand natural photosynthesis and construct artificial LH systems.

Tubular chlorophyll aggregates could be prepared through mimicking the self-assembly system in a chlorosome *via* hydrogen bonds, coordination bonds, and π-stackings.[8,12–14] However, ring-shaped chlorophyll self-aggregates, such as an arrangement in LH1/2, have not been constructed. Herein, we report the formation of a circular supramolecular polymer by the self-assembly of naphthalenediamide-linked chlorophyll dimers. The dimeric compound is self-assembled in a nonpolar organic solvent to readily produce wavy nanofibers. Some nanofibers in dispersion were transformed into ring-shaped supramolecular polymers without any scaffolds after several hours. We envision that the chlorophyll nanoring has the potential for a new type of LH antenna model which could be applied to artificial photosynthesis and solar cells.

In a previous study, we reported the construction of linear supramolecular polymers through columnar stacking by hydrogen bonds and π-stackings using a benzenediamide-linked chlorophyll dimer.[15] Yagai's group have successfully constructed curved or ring-shaped supramolecular polymers by slipped stacking of disk-like components which are called "rosettes".[16–18] We designed naphthalenediamide-linked chlorophyll dimer **1** (Fig. 1a) to expect curved stacking as inspired by these strategies. Compound **1** was synthesized by condensation with a chlorophyll-*a* derivative possessing an amino group at the 3^1-position with 1,4-naphthalenedicarbonyl dichloride (detailed procedures are provided in the ESI†).[15] Synthetic dyad **1** was fully characterized by UV-visible absorption, ^{1}H and ^{13}C NMR, and mass spectra (see ESI†).

To study the optical properties of chlorophyll dimer **1**, its UV-visible absorption and circular dichroism (CD) spectra in $CHCl_3$ and 5% (v/v) $CHCl_3$–hexane were measured (Fig. 1b). The spectrum of **1** in $CHCl_3$ showed sharp and strong peaks at 412 and 666 nm, called Soret and Qy bands, respectively, where small CD signals were obtained (Fig. 1b, black lines). These data indicated that **1** was monomeric in $CHCl_3$. In contrast, 5% (v/v) $CHCl_3$–hexane of **1** exhibited slightly shifted and broadened visible absorption peaks and relatively intense CD Cotton effects (Fig. 1b, red lines). Fourier transform infrared (FT-IR) spectra of **1** dissolved in $CHCl_3$ and dispersed in 5% (v/v) $CHCl_3$–hexane were also measured, and their specific spectra are displayed in Fig. 1c.[15] The FT-IR peak at 3432 cm^{-1} and shoulder of ≈1655 cm^{-1} attributed to 3^1-N–H and 3^2-C=O stretching bands, respectively, of monomeric **1** in $CHCl_3$ were shifted to lower wavenumbers at ≈3250 and 1626 cm^{-1} in 5% (v/v) $CHCl_3$–hexane. These spectral changes in UV-vis absorption, CD, and FT-IR indicate that dimer **1** formed self-aggregates by hydrogen bonds between amido groups at the 3^1-position as well as π–π interaction of chlorin moieties.

[a] *Graduate School of Life Sciences, Ritsumeikan University, Kusatsu, Shiga, 525-8577, Japan. E-mail: tamiaki@fc.ritsumei.ac.jp*
[b] *Graduate School of Engineering, Nagoya Institute of Technology, Nagoya, Aichi, 466-8555, Japan. E-mail: matsubara.shogo@nitech.ac.jp*

† Electronic supplementary information (ESI) available. See DOI: https://doi.org/10.1039/d2cc06368a

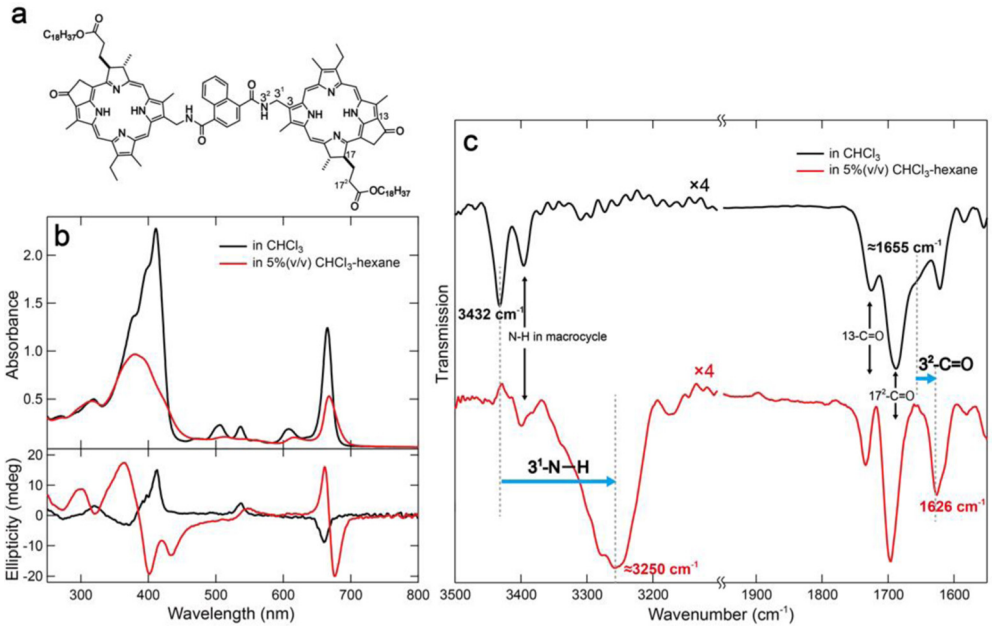

Fig. 1 (a) A chemical structure of naphthalene-liked chlorophyll dimer **1**. (b) UV-vis absorption (upper) and CD spectra (lower) of dimer **1** (10 μM) in $CHCl_3$ (black) and 5% (v/v) $CHCl_3$–hexane (red). (c) FT-IR spectra of dimer **1** (1 mM) in $CHCl_3$ (black) and 5% (v/v) $CHCl_3$–hexane (red).

The self-aggregates of dimer **1** prepared in 5%(v/v) $CHCl_3$–hexane were observed by atomic force microscopy (AFM) in characterizing their morphology. The AFM samples of assembled **1** were prepared by casting the suspension on highly oriented pyrolytic graphite (HOPG) and spin-coating. The AFM image of self-aggregates of **1** just after preparation of the suspension presented nanofibers with a height of ≈2.5 nm (Fig. 2a, c, red line and Fig. S6a, c, red lines, ESI†). The height of the nanofiber was comparable to the estimated molecular distance, which was the long axis along a chlorophyll–naphthalene–chlorophyll π-skeleton (Fig. 2d), suggesting that the nanofiber was constructed by columnar stacking of dimer **1** in the same fashion as the previous study.[15]

Interestingly, circular nanostructures were observed in the AFM image of assembled **1** after standing the suspension for one day (Fig. 2b and Fig. S6b, ESI†). The diameters of ring-shaped aggregates range from 50 to 600 nm and the corresponding circumferences are approximately 160–1900 nm (Fig. S5, ESI†). The lengths of the wavy nanofibers are almost comparable to the circumferences. The height of the nanorings is the same as that of the wavy nanofibers (≈2.5 nm) (Fig. 2c and Fig. S6c, blue lines, ESI†). These matches imply that the fiber-like aggregates of **1** were transformed into ring-shaped supramolecules. We presumed that the curvature of the aggregates was attributed to slipped stackings of chlorophyll dimer **1** occurring with twisted hydrogen bonds between amide groups due to steric hindrance at the naphthalene moiety.[16–19] In contrast to the wavy nanofiber of **1**, benzene-linked dimer $\mathbf{1_{Bn}}$ formed straight and long nanofibers by vertical stackings of $\mathbf{1_{Bn}}$ (Fig. S7, ESI†).[15] In addition, an elongation of the terminals of the bent nanofiber led to cyclization and gave an end-to-end closed nanoring.[19] The assembling fashion of the nanoring was

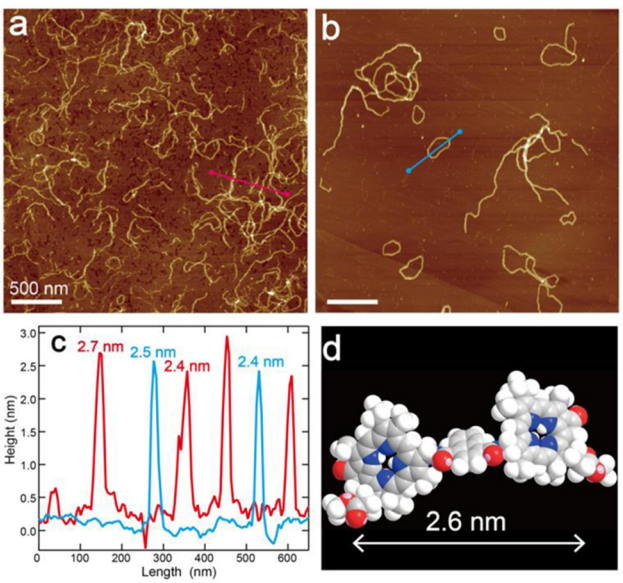

Fig. 2 AFM images of assembled dimer **1** just after preparation of suspension (a) and after standing the suspension for 1 day (b). The concentration of **1** in the AFM samples was 10 μM. All the white bars show a 500 nm length. (c) Height profiles along the red-line in (a) and the blue-line in (b). (d) Optimized molecular structure of **1** using MM2 calculation. The stearyl esters at the 17^2-position of the chlorophyll moieties were replaced by the methyl esters to calculate the π-core model.

much the same as that of the wavy nanofiber to show similar UV-vis absorption and CD spectra (Fig. S4, ESI†), even though the morphology of these aggregates was varied with time.

We conducted a time-dependent AFM observation of self-aggregates of chlorophyll dimer **1** to investigate the cyclization mechanism. In the AFM sample of assembled **1** after standing

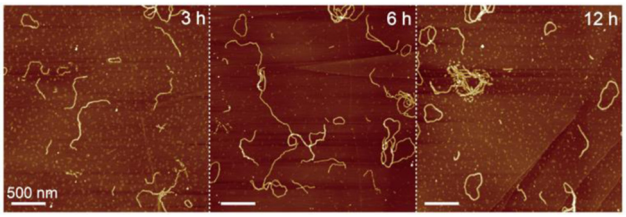

Fig. 3 AFM images of assembled dimer **1** after standing the suspension (10 μM) for 3 (left), 6 (middle), and 12 h at room temperature (right).

the suspension for 3 h, ring-shaped aggregates were occasionally found, while most of the aggregates were fiber-shaped (Fig. 3a, left). The number of nanorings increased with decreasing nanofibers from the AFM image of the self-aggregates after standing for 6 h (Fig. 3a, middle). An AFM image of assembled **1** after 12 h mainly showed nanorings (Fig. 3a, right) and the one-day standing sample (Fig. 2b). According to the percentages of nanoring comparing all the assembled dimer **1**, which were determined by counting the numbers of nanostructures in the AFM images (Table S1, ESI†), the ratio of ring-shaped aggregates increased with time. This result indicates that metastable fiber-like aggregates transformed into thermodynamically stable nanorings.

Transformations from the metastable state into thermodynamically stable aggregates are often observed in supramolecular polymers including chlorophyll aggregates, which are dependent on temperature and concentration.[17,20–23] To further investigate the transformation, we demonstrate the thermo- and concentration-dependent AFM analysis. Wavy nanofibers of **1** hardly transformed into nanorings by standing the suspension for 3 h at room temperature (Fig. 3, left). However, the cyclization was facilitated at 50 °C and most of the aggregates were converted to ring-shaped nanostructures after standing for just 3 h (Fig. 4a). From the AFM image of low-concentrated (1 μM) aggregates of **1**, several nanorings were observed immediately after the sample preparation (Fig. 4b). On the contrary, ring-shaped aggregates were rarely found in the highly concentrated (100 μM) dispersion of **1** (Fig. S8, left, ESI†), and the transformation into network aggregates occurred by standing the dispersion for one day (Fig. S8, right, ESI†). According to the results, we assumed that the heating process induced a disassembly of the wavy nanofibers to generate short nanofibers that act as a precursor of nanofibers and promoted a cyclization. At low concentrations, the ring-shaped aggregates were obtained by preferential end-to-end elongation within a single supramolecule (Fig. 4c, right), while the end-to-end linkage between nanofibers was preferential at high concentrations and gave network nanostructures (Fig. 4c, left).

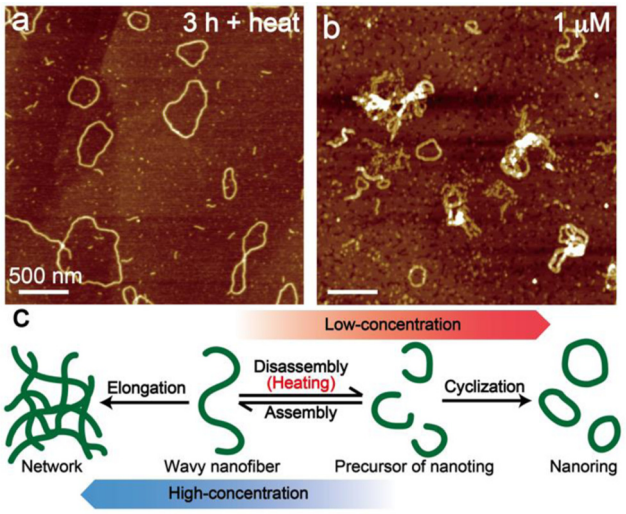

Fig. 4 AFM images of assembled dimer **1**: (a) after standing the suspension (10 μM) for 3 h at 50 °C; (b) just after preparation of the low-concentrated dispersion (1 μM). (c) Schematic model of two possible elongation pathways for the formation of network and ring-shaped aggregates.

Finally, we demonstrated the isolation of ring-shaped supramolecular aggregates of chlorophyll dimer **1**. Dispersion of assembled **1** at a concentration of 10 μM after standing for one day was filtrated by using a membrane filter with a 0.45 μm pore size. The dispersion of assembled **1** included large amorphous aggregates as minor species whereas ring-shaped aggregates were mainly observed (Fig. 2b and Fig. S6a, ESI†). After filtration of the suspension, large aggregates (hydrodynamic diameter $>$ 3 μm) disappeared in the filtrate from dynamic light scattering measurements (Fig. S9a, ESI†), and relatively uniform nanorings (an appropriate 0.2 μm size) were observed from the AFM image after spin coating the filtrate on a HOPG substrate (Fig. S9b, ESI†). The short nanofibers and small nanoparticles could not be removed, but rough purification of circular aggregates was feasible.

In summary, we constructed ring-shaped supramolecular aggregates which mimicked the molecular arrangement in LH1/2 without any scaffolds. The naphthalenediamide-linked chlorophyll dimers self-assembled to form metastable aggregates with wavy- and fiber-shapes, and then the wavy nanofibers transformed into ring-shaped supramolecules by time course and heating. The nanorings of chlorophyll aggregates are expected to be useful for artificial LH systems and to elucidate the physical properties in photosynthesis. Further investigations on the optical properties of the nanoring are underway.

This work was partially supported by the Japan Society for the Promotion of Science (JSPS) KAKENHI Grant Number 22H02203 (to H. T.).

Conflicts of interest

There are no conflicts to declare.

Notes and references

1 T. Mirkovic, E. E. Ostroumov, J. M. Anna, R. van Grondelle, Govindjee and G. D. Scholes, *Chem. Rev.*, 2017, **117**, 249–293.
2 H. Lokstein, G. Renger and J. P. Götze, *Molecules*, 2021, **26**, 3378.
3 G. McDermott, S. M. Prince, A. A. Freer, A. M. Hawthornthwaite-Lawless, M. Z. Papiz, R. J. Cogdell and N. W. Isaacs, *Nature*, 1995, **374**, 517–521.

4 A. W. Roszak, T. D. Howard, J. Southall, A. T. Gardiner, C. J. Law, N. W. Isaacs and R. J. Cogdell, *Science*, 2003, **302**, 1969–1972.
5 L.-J. Yu, M. Suga, Z.-Y. Wang-Otomo and J.-R. Shen, *Nature*, 2018, **556**, 209–213.
6 P. Qian, D. J. K. Swainsbury, T. I. Croll, P. Castro-Hartmann, G. Divitini, K. Sader and C. N. Hunter, *Biochemistry*, 2021, **60**, 3302–3314.
7 G. T. Oostergetel, H. van Amerongen and E. J. Boekema, *Photosynth. Res.*, 2010, **104**, 245–255.
8 S. Matsubara and H. Tamiaki, *J. Photochem. Photobiol. C: Photochem. Rev.*, 2020, **45**, 100385.
9 J. Huh, S. K. Saikin, J. C. Brookes, S. Valleau, T. Fujita and A. Aspuru-Guzik, *J. Am. Chem. Soc.*, 2014, **136**, 2048–2057.
10 N. P. D. Sawaya, J. Huh, T. Fujita, S. K. Saikin and A. Aspuru-Guzik, *Nano Lett.*, 2015, **15**, 1722–1729.
11 X. Li, F. Buda, H. J. M. de Groot and G. J. A. Sevink, *iScience*, 2022, **25**, 103618.
12 S. Sengupta, D. Ebeling, S. Patwardhan, X. Zhang, H. von Berlepsch, C. Böttcher, V. Stepanenko, S. Uemura, C. Hentschel, H. Fuchs, F. C. Grozema, L. D. A. Siebbeles, A. R. Holzwarth, L. Chi and F. Würthner, *Angew. Chem., Int. Ed.*, 2012, **51**, 6378–6382.
13 S. Shoji, T. Ogawa, T. Hashishin, S. Ogasawara, H. Watanabe, H. Usami and H. Tamiaki, *Nano Lett.*, 2016, **16**, 3650–3654.
14 S. Matsubara and H. Tamiaki, *J. Am. Chem. Soc.*, 2019, **141**, 1207–1211.
15 S. Matsubara and H. Tamiaki, *Chem. Lett.*, 2021, **50**, 999–1001.
16 S. Yagai, Y. Goto, X. Lin, T. Karatsu, A. Kitamura, D. Kuzuhara, H. Yamada, Y. Kikkawa, A. Saeki and S. Seki, *Angew. Chem., Int. Ed.*, 2012, **51**, 6643–6647.
17 S. Yagai, Y. Kitamoto, S. Datta and B. Adhikari, *Acc. Chem. Res.*, 2019, **52**, 1325–1335.
18 S. Takahashi and S. Yagai, *J. Am. Chem. Soc.*, 2022, **144**, 13374–13383.
19 G. Ouyang, L. Ji, Y. Jiang, F. Würthner and M. Liu, *Nat. Commun.*, 2020, **11**, 5910.
20 S. Ogi, C. Grzeszkiewicz and F. Würthner, *Chem. Sci.*, 2018, **9**, 2768–2773.
21 S. Matsubara and H. Tamiaki, *ACS Appl. Nano Mater.*, 2020, **3**, 1841–1847.
22 S. Yagai, S. Kubota, H. Saito, K. Unoike, T. Karatsu, A. Kitamura, A. Ajayaghosh, M. Kanesato and Y. Kikkawa, *J. Am. Chem. Soc.*, 2009, **131**, 5408–5410.
23 S. Matsubara and H. Tamiaki, *Photosynth. Res.*, 2020, **145**, 129–134.

